doi:10.20944/preprints202008.0599.v1

Preparation of PP-g-(AA-MAH) Fibers using Suspension Grafting and Melt-blown Spinning and its Adsorption for Aniline in Wastewater

Zhouyang Lian[1*], Yiyang Xu[1], Jie Zuo[1], Hui Qian[1], Zhengwei Luo[2], Wuji Wei[1]

[1] School of Environmental Science and Engineering, Nanjing Tech University, Nanjing, China.
[2] School of Biotechnology and Pharmaceutial Engineering, Nanjing Tech University, Nanjing, China.
[*] Correspondence: lianzy@njtech.edu.cn

Abstract: This paper uses polypropylene (PP) as the matrix and acrylic acid (AA) and maleic anhydride (MAH) as functional monomers to prepare PP-g-(AA-MAH) fibers by suspension grafting and melt-blown spinning technology that are easy to industrially scale-up. The fibers can be used to adsorb aniline from wastewaters. Results showed that the grafting ratio reached the maximum of 12.47%. The corresponding optimal conditions were grafting time of 3h, AA : MAH = 0.75, total monomer content of 55%, benzoyl peroxide 1.4%, xylene concentration of 6 mL/g PP, and deionized water content of 8 mL/g PP. Owing to its good fluidity and thermal stability, the product of suspension grafting can be used for melt-blown spinning. Infrared spectroscopic and nuclear magnetic resonance spectroscopic analyses indicated that AA and MAH were successfully grafted onto PP fibers. After grafting, the hydrophilicity of PP-g-(AA-MAH) fiber increased. Therefore, it had higher adsorptivity for aniline and the adsorption capacity could reach 42.2 mg/g at 45 min. Moreover, the PP-g-(AA-MAH) fibers showed good regeneration performance.

Keywords: polypropylene; suspension grafting; melt-blown spinning; adsorption; aniline

1 Introduction

Water discharged from industrial activities, if left untreated or is not treated up to proper standard, inevitably causes water pollution, which is one of the major environmental issues of the day[1,2]. Aniline is one of the common organic compounds, used as an intermediate in chemical industry, and hence its market demand has risen sharply[3-5]. This provides more channels for aniline to enter water bodies, thus causing environmental pollution. Data[6-9] shows that in China itself, annually, nearly 30,000 tons of aniline enters the water bodies, through various pollution routes. In the United States, on an average about 600,000 tons of aniline-containing wastewater is discharged into the environment annually, whereas in Europe, this figure is about 1.4 times that of the United States. Since aniline does not readily undergo degradation, it accumulates in the environment. Moreover, being carcinogenic, teratogenic, mutagenic and highly toxic substance, aniline has a severely high risk of causing potential damage to the environment and organisms[10-12]. Therefore, aniline has been included in the list of preferentially-controlled pollutants by Minister of Ecology and Environment of China, the United States Environmental Protection Agency, European Chemicals Agency, and other agencies[13-15].

At present, treatment methods for aniline-containing wastewaters mainly include advanced oxidation[16,17], membrane separation[18,19], extraction[20,21], biological methods[22], and adsorption methods[23-26]. Among them, the adsorption method that uses the interactions between adsorbent and adsorbate to remove pollutants from wastewater has attracted the attention of researchers, because of its simple operation, fast processing, and resourceful recovery[27]. Especially for treating sudden incidents of water pollution, adsorption method is considered as the first choice, owing to its high efficiency. Therefore, development of adsorbents using a wide range of raw materials, at low price, and achieving strong adsorption capacity through simple post-adsorption treatment of aniline wastewater has become the focus of research[28].

Polypropylene (PP) is acid- and alkali-resistant, very common material, cheap, and easy to process. After PP is spun by melt-blowing into fibers, it forms a three-dimensional network structure, with smaller mono-filament diameter, higher porosity, and larger specific surface area[29-31]. Therefore, it has been widely used as a matrix fiber. However, since PP is non-polar in nature, it does not possess polar and reactive groups along its molecular chains, which limits its ability to adsorb pollutants from wastewaters[32]. Our research group has been actively involved in the preparation of functionalized PP fibers with special properties through grafting, chemical modification, and other methods[33-35].

Suspension grafting[36] is a new, environment-friendly, and easy-to-industrialize method for grafting modification. This method usually employs water as the dispersion medium and polymer particles as the dispersed phase. It forms a suspension system, under the action of shear force provided by mechanical stirring. Each suspended polymer particle can be regarded as an independent "reaction bed". Within this "reaction bed", the functional monomers undergo graft polymerization under the action of initiators. This polymerization method has advantages of high reaction efficiency, few side reactions, and simple post-processing of products. Li[37] et al. prepared PP-g-PMMA with water as the dispersant and dibenzoyl peroxide as the initiator using the suspension grafting method. The addition of a second monomer, styrene, increased the grafting ratio of monomer to 24.5%. This indicated an effective improvement in the compatibility of PP/ASA mixture.

In this study, the amorphous region of PP was first expanded by quenching treatment, and then functional monomers like acrylic acid (AA) and maleic anhydride (MAH) were grafted onto the surface of PP by suspension grafting. Finally the PP-g-(AA-MAH) fibers were prepared by melt-blown spinning technology. The adsorption and regeneration performance of PP-g-(AA-MAH) fibers for aniline in wastewaters were investigated.

2 Experimental

2.1 Experimental materials

PP resin especially for melt-blown process was provided by Shanghai Expert New Material Co. Ltd. Other chemical reagents, such as AA, MAH, xylene, benzoyl peroxide (BPO), acetone, absolute ethanol, sodium hydroxide, hydrochloric acid, etc. were all analytically pure and commercially available.

2.2 Preparation of PP-g-(AA -MAH) fibers

A certain amount of PP resin and xylene were charged into a magnetically-stirred reactor and the temperature was raised to 140 °C under stirring. Then, a certain amount of deionized water was rapidly pumped at normal temperature into the reactor to cool down the temperature of the reaction mixture. After this, the temperature of the reactor was maintained at 90 °C and then the mixture was allowed to swell for 30 minutes. Then, the monomers AA and MAH and BPO initiator were added to the reaction kettle through the high-pressure feed port and graft polymerization was carried out for a certain period of time under strong stirring. The obtained products were washed with deionized water and acetone to remove unreacted monomers and homopolymers. The washed product was dried and then passed through a melt-blown spinning machine[38] to obtain PP-g-(AA-MAH) fibers.

2.3 Calculation of grafting ratio

PP-g-(AA-MAH) fibers (0.5 g) were placed in a 250 mL round-bottom flask. Xylene (100 mL) and sodium hydroxide-ethanol solution (0.05 mol/L, 30 mL) were added in succession. The mixture was allowed to boil at 120 °C for 30 min. After the solution was cooled to room temperature, 3-5 drops of thymol blue indicator was added and then the mixture was titrated with hydrochloric acid-isopropanol solution (0.05 mol/L) until the blue color just disappeared. The ungrafted PP fibers were used as the blank sample for comparison. The grafting ratio was calculated as follows:

$$G_p\% = \frac{(V_0-V_1)\times C\times(98.06+72.06)}{3\times m}\times 100\% \qquad （1）$$

where G_p(%) denotes the grafting ratio; V_0(L) and V_1(L) represent the volumes of HCl-isopropanol solution consumed to titrate PP fibers and PP-g-(AA-MAH) fibers, respectively; C(mol/L) denotes the concentration of HCl-isopropanol solution; m denotes the mass of the fiber sample (g); 98.06 g/mol and 72.06 g/are the molar masses of MAH and AA, respectively.

2.4 Characterization methods

X-ray diffractometer (X'TRA) was used to characterize the crystal structures of sample before and after quenching. The fluidity and thermal stability of the suspension grafting product were studied by melt indexer (RL-Z1B1) and thermal analyzer (Pyris 1 DSC), respectively. The functional groups of the modified fibers were analyzed using Fourier transform infrared spectrometer (Nexus 670) and nuclear magnetic resonance spectrometer (DRX500).

2.5 Hydrophilicity of PP-g-(AA-MAH) fiber

The Washburn equation[39] can determine the contact angle of a dynamic liquid by measuring the speed at which the liquid penetrates into the filled powder (Eqn. 2). However, the penetration height of wetting liquid is difficult to determine. As the penetration height changes, the air in the capillary tube gets compressed and the air pressure increases[40]. Therefore, Eqn. 2 can be revised by the relationship between osmotic pressure and height and Eqn. 3 is obtained.

Let $K_\theta = \frac{\beta\gamma_{LV}\cos\theta}{\eta}$

K_θ can be obtained from the linear relationship between $(\Delta P)^2$ and t.

In this study, the water contact angle of degreased cotton with good hydrophilicity was set to 0, that is, when $\theta = 0$, then the equation becomes $K_0 = \frac{\beta\gamma_{LV}}{\eta}$. Since the bulk densities of all the test samples was almost the same and deionized water was used as the wetting liquid, the β, η, and γ_{LV} values of the test samples were approximately the same. Due to these similarities, Eqn. 4 can be obtained for calculating the water contact angle on the surface of tested fiber. The schematic diagram of the self-made device is shown in Figure 1.

$$h^2 = \frac{R_{eff}\,\gamma_{LV}\cos\theta}{2\eta}t \qquad (2)$$

$$(\Delta P)^2 = \frac{\beta\gamma_{LV}\cos\theta}{\eta}t \qquad (3)$$

$$\theta = \arccos\left(\frac{K_\theta \eta}{\beta\gamma_{LV}}\right) = \arccos\left(\frac{K_\theta}{K_0}\right) \qquad (4)$$

where h denotes the penetration height of the wetting liquid in time t; R_{eff} denotes the effective capillary radius; γ_{LV} denotes the surface tension of the wetting liquid; θ denotes the water contact angle; η denotes the viscosity of the wetting liquid; t denotes the penetration time; ΔP denotes the change in osmotic pressure, and β denotes the parameters related to the stacking mode of the stacked bed.

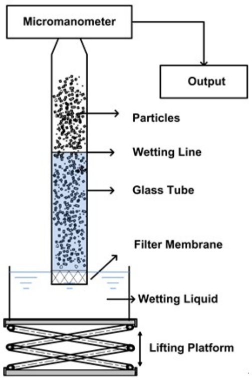

Figure 1.The schematic diagram of the self-made device

2.6 Adsorption and desorption of aniline by PP-g-(AA -MAH) fiber

A certain amount of PP-g-(AA-MAH) fibers was taken in a conical flask containing aniline solution to achieve a concentration of 300 mg/L, as that of simulated wastewater. After adsorption at 25 °C under shaking, the fibers were taken out. After allowing to stand for 5 minutes, the aniline concentration was determined and the adsorption capacity was calculated from equation.

$$Q = \frac{(C_0 - C_1)V}{m} \tag{5}$$

where Q (mg/g) denotes the adsorption capacity; C_0 (mg/L) and C_1 (mg/L) denote the concentrations of aniline in the solution before and after adsorption; V (L) denotes the volume of the solution; and m (g) is the mass of fiber as absorbent.

The adsorption-saturated PP-g-(AA-MAH) fiber was desorbed by shaking in 0.5 mol/L HCl solution for a certain period of time. The concentrations of aniline in the solution were measured at different times and the desorption ratios were calculated from Eqn. 6.

$$D = \frac{CV}{mQ} \times 100\% \tag{6}$$

where D (%) denotes the desorption ratio; C denotes the concentration of aniline in the eluent (mg/L); Q is the adsorption capacity of the fiber (mg/g); V is the volume of the eluent (L), and m denotes mass of fiber (g).

3 Results and discussion

3.1 The mechanism of suspension grafting polymerization of two monomers

The schematic diagram for the mechanism of suspension grafting polymerization of AA and MAH monomers[33] is shown in Figure 2. In the suspension grafting reaction system, under the action of shear force provided by high-speed stirring, each PP resin particle swelled up and was surrounded by xylene. It dispersed into an independent "reaction bed" in deionized water as the dispersant. The grafting polymerization in each "reaction bed" mainly occurred in the amorphous regions of PP resin. In this study, PP resin was quenched before the graft polymerization, in order to enlarge the amorphous region and PP transformed from a resin to a particle with surface micropores. The swelling effect could not only expand the amorphous region further but also enabled the BPO initiator and AA and MAH monomers to diffuse through the surface and into the pores of PP particles more uniformly. Especially, under the action of xylene, they could migrate to the internal micropores of PP more conveniently.

Generally, the initiator first decomposes to form primary free radicals. The primary free radicals can generate PP macromolecular free radicals denoted as α, by capturing α-H from the PP molecular chains (Reaction 1). The macromolecular free radicals, α, react with monomers to form the target product, ε (Reaction 3). However, side reactions like homo-polymerization of monomers (Reaction 4) and PP degradation (Reaction 2), also occur during this process. In the presence of AA, AA first attacks the PP macromolecular radicals α during the grafting polymerization, since AA is an electron provider and has higher reactivity. It can rapidly react with the PP macromolecular radicals α. Moreover, it inhibits side reactions like degradation to form stable PP-AA macromolecular free radicals. The macromolecular free radicals further react with AA or MAH, which is the main reaction pathway. At the same time, due to low reaction temperature, it becomes difficult for the degradation products to react with the monomer (Reaction 5).

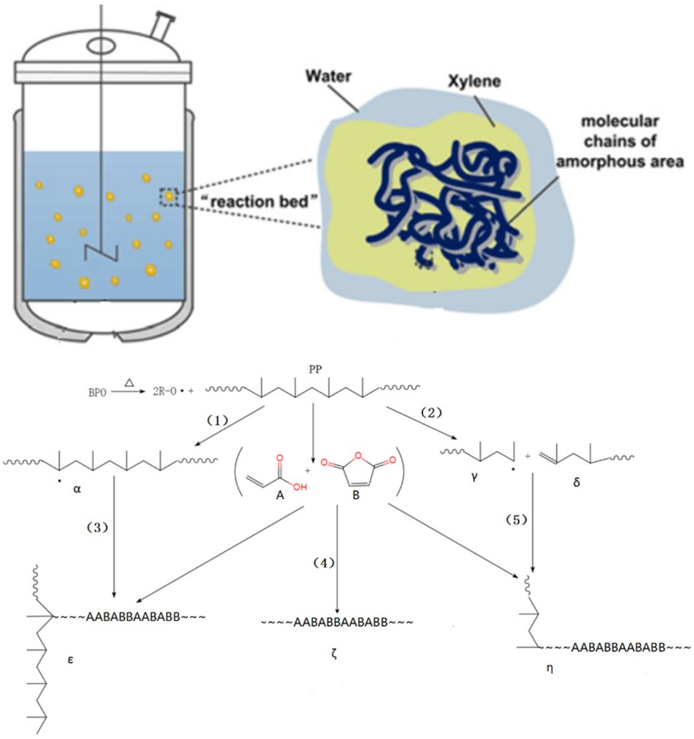

Figure 2. The schematic diagram for the mechanism of suspension grafting polymerization of AA and MAH monomers

3.2 Effect of quenching treatment

The PP used in this research is a special raw material for melt-blown process. It has high crystallinity, but the suspension grafting modification is mainly carried out in the amorphous regions of PP. Therefore, the PP melt can be quenched to reduce its crystallinity, which makes the grafting polymerization easier. It can be seen from the X-ray diffraction patterns of PP before and after the quenching treatment in Fig. 3 that the dispersion peak intensity (shaded area in the figure) of the amorphous region of the quenched PP was significantly greater than that of the original PP. Since the quenching process greatly shortens the crystallization time of PP melt, some of the PP macromolecular chains have no time to move, transform from the disordered coils and then grow into crystals, which results in lower crystallinity.

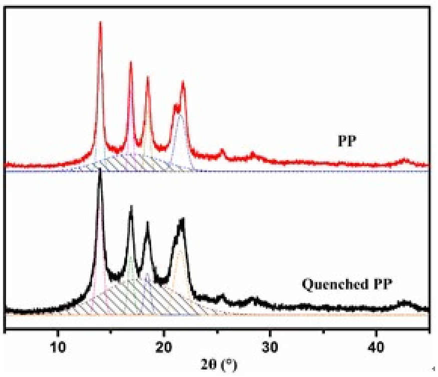

Figure 3. X-ray diffraction patterns of PP before and after the quenching treatment

3.3 Effects of different parameters on grafting ratio in suspension grafting polymerization

The main factors affecting grafting in suspension grafting polymerization include the grafting time, the AA/MAH ratio, the total amount of monomers, and the dosages of BPO, xylene, and deionized water. Therefore, effects of the six factors on the grafting ratio were all investigated and the results are shown in Figure 4.

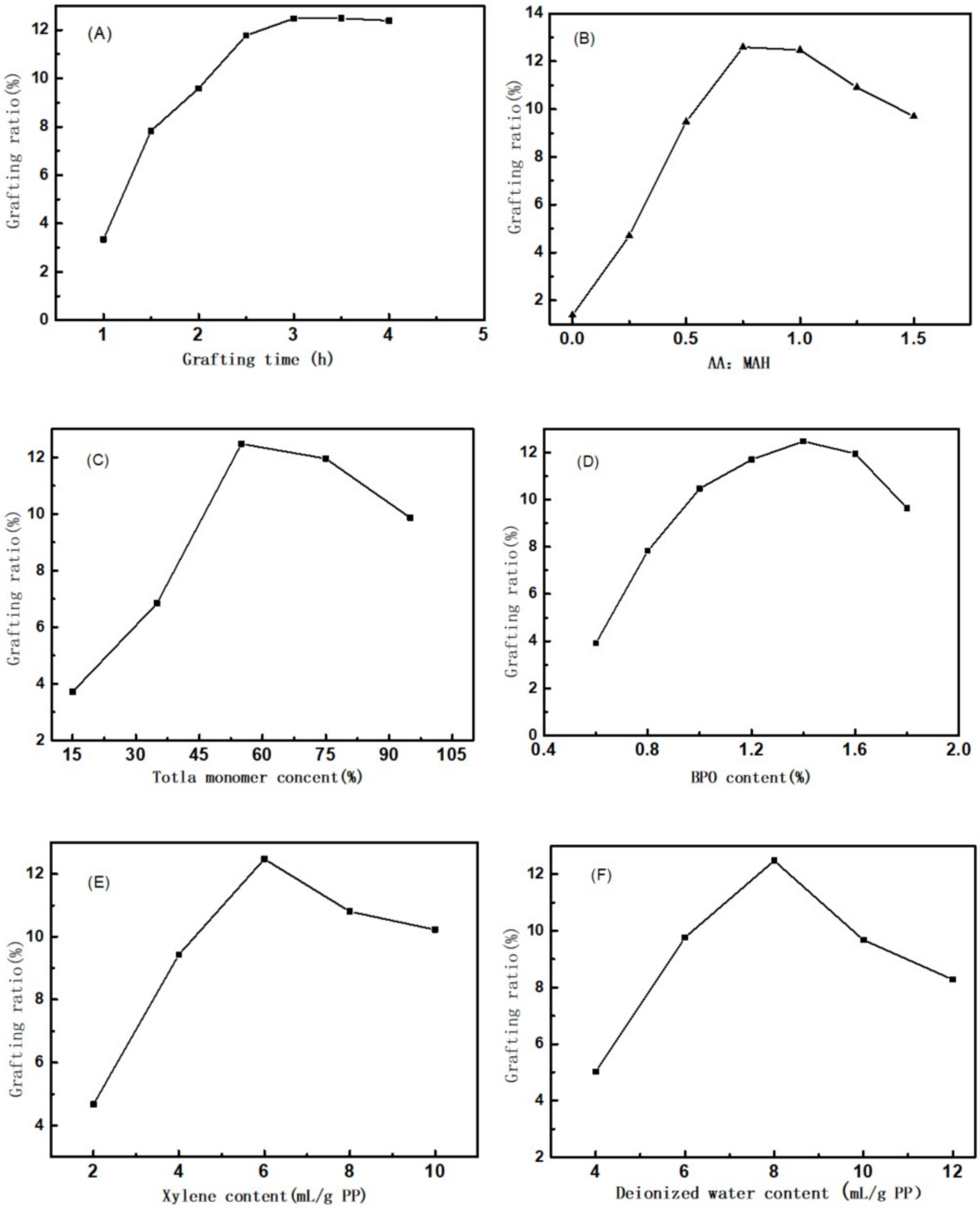

Figure 4. Effects of grafting time (A), AA/MAH ratio (B), total monomer content (C), and the dosages of BPO (D), xylene (E), and deionized water (F) on grafting ratio

It can be seen from Figure 4A that the grafting ratio increased rapidly with increase in grafting time and it reached a stable state after 3 hours. The half-life period of the initiator BPO at 90 °C is 1 h[33]. In the initial stages of the reaction, BPO decomposed into a large number of primary free radicals, which rapidly initiated the grafting reaction. In addition, the monomer concentration was also high at this time, due to which the grafting ratio increased rapidly. After 3h, BPO was basically decomposed and the monomer concentration was also lower, exhibiting a more stable grafting ratio.

From Figure 4B it was evident that when the mass fraction of AA was 0, the grafting ratio was only 1.38%. Subsequently, as the AA/MAH ratio increased, the grafting ratio increased at first and then decreased. With increase in the amount of monomer AA added, the concentration of macromolecular free radicals with AA chains increased. This increased the probability of free radicals contacting with PP. In addition, the monomer MAH could not undergo self-polymerization, due to its steric hindrance. When AA was added, it could form a copolymer with MAH and then graft with the PP segment[41], due to which the grafting ratio increased. However, as the amount of AA added continued to increase, the probability of capturing primary free radicals increased, thereby forming more number of AA-containing macromolecular free radicals. The probability of termination due to recombination between these free radicals increased, which resulted in lower grafting ratio. In addition, more the number of AA molecules, more was the probability of AA initiation, which then reduced the probability of formation of macromolecular free radicals of PP, thereby affecting the grafting ratio.

It can be seen from Figure 4C that as the total amount of monomers AA and MAH increased, the grafting ratio increased at first and then decreased. Higher monomer concentration increased the effective collisions between the monomers and PP macromolecular radicals, thereby increasing the grafting ratio. However, grafting polymerization mainly occurred in the amorphous regions of PP. Although the amorphous regions of PP expanded after quenching, the reaction space was still limited. Too high monomer concentration led to more homopolymerization as the side reaction. Additionally, the mass transfer of monomer and initiator were also affected, so the grafting ratio decreased.

With increase in the amount of initiator BPO, the grafting ratio first increased and then decreased. When the amount of added BPO accounted for 1.4% of PP, the grafting ratio reached the maximum value of 12.47% (Figure 4D). On heating, BPO first decomposed into benzoyl radicals. Due to steric hindrance, benzoyl radicals were further decomposed into benzene radicals with stronger capability for H atom. Benzene radicals flowed and diffused slowly in the PP particles within limited space, depriving the α-H from the PP chains to form PP macromolecular radicals and initiating monomer polymerization. Therefore, by appropriately increasing the amount of BPO more number of benzene radicals could be generated. This increased the number of monomers participating in the grafting reaction and increased the grafting ratio. However, excessively high concentration of benzene radicals could cause explosive polymerization and lead to an increase in homopolymerization side reactions. This would again affect the progress of the grafting reaction and also result in degradation of PP[42].

It can be seen from Figure 4E that with the increase in amount of xylene, the grafting ratio increased rapidly and then decreased slightly. With xylene concentration of 6 mL/g PP, the grafting ratio reached the maximum value of 12.47%. The monomers used in this study possessed polar groups, and hence their solubility parameters were quite different from that of PP, which implied lower swelling capability of PP. The addition of certain amount of xylene helped to increase the swelling degree of PP and provided greater space for the grafting reaction. Meanwhile, the addition of xylene also kept the concentration of water-soluble monomers at the interface to a low level. This effectively reduced homo-polymerization as side reaction and increased the grafting ratio. However, too much of xylene readily formed a film covering the surface of PP, which hindered the grafting reaction between monomer and PP and affected the grafting ratio.

Figure 4F shows that as the amount of deionized water as dispersant increased, the grafting ratio increased rapidly and then decreased. As the amount of deionized water reached 8 mL/g PP, the grafting ratio reached the maximum value. If the amount of deionized water added was too less, the dispersion of PP into multiple independent "reaction beds" became difficult, since PP particles agglomerated in the reactor to form agglomerates, resulting in a low grafting ratio. With too much of deionized water, although the PP particles could form numerous independent "reaction beds", the concentration of monomer dissolved in the water decreased. Hence, the monomer concentration gradient between the dispersion medium and the interfacial reaction layer became smaller. As a result, it was difficulty for the monomer molecules to enter the interfacial layer and participate in the grafting polymerization reaction, due to which the grafting ratio decreased.

3.4 Effect of suspension grafting on the performance of melt-blown spinning product

Melt-blown spinning has strict requirements of fluidity and thermal stability of raw materials. PP resin itself has greater fluidity, but after its modification with polar groups, the interactions between molecular chains increase and the fluidity is affected. In addition, in the melt-blown spinning process, the raw materials are melted at high temperature and extruded through the screw. Hence, only better thermal stability can ensure that no decomposition of the raw materials occurs during the process. Therefore, the melt flow-rate (MFR) and thermogravimetric (TG) of PP and PP-g-(AA-MAH) were investigated to determine whether it can be spun into fibers. The results are presented in Figure 5.

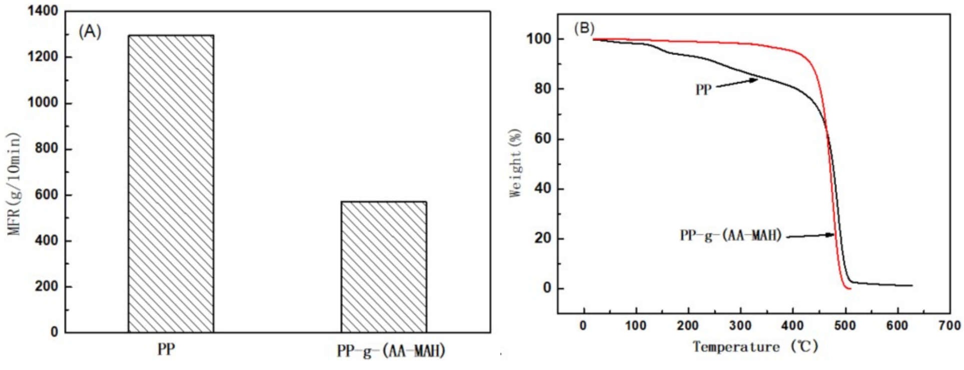

Figure 5. MFR (A) and TG (B) of PP and PP-g-(AA-MAH) fibers

It can be seen from Figure 5A that MFR (570 g/10 min) of the product PP-g-(AA-MAH) of suspension grafting was lower than that of the PP raw material (1296 g/10 min), implying decrease in fluidity. However, the MFR was still higher than that required for the melt-blown process of PP melt (400 g/10 min). The decrease in MFR could be attributed mainly to the strengthening of hydrogen bonds between the grafted polar chains[33,38]. Compared with the TG curves of unmodified PP in Figure 5B, the product of suspension grafting PP-g-(AA-MAH) had better thermal stability. PP-g-(AA-MAH) showed no significant weight loss before 250 °C, and hence the melt-blown spinning at maximum temperature of 220 °C basically did not cause decomposition.

3.5 Characterization of fibers

3.5.1 Fourier transform infrared analysis (FT-IR)

PP and its products of suspension grafting - PP-g-AA, PP-g-MAH, and PP-g-(AA-MAH) were spun by melt-blowing and processed into fibers. Their FTIR spectra (the total monomer contents were the same during the suspension grafting process) are shown in Figure 6. The fibers of modified PP-g-AA, PP-g-MAH, and PP-g-(AA-MAH) showed unique characteristic absorption peaks of PP, viz. symmetrical (2924 cm^{-1}) and asymmetrical (2842 cm^{-1}) C-H stretching vibrations of $-CH_3$, the flexural vibrations of $-CH_2-$ at 1380 cm^{-1}, and absorption of C-H at 1450 cm^{-1}. Compared with that of PP fiber, the FTIR spectrum of PP-g-AA fiber showed peak for C=O stretching vibrations of the carboxyl group (1720 cm^{-1}), indicating the successful grafting of AA onto the PP chain. Compared to the spectrum of PP fiber, PP-g-MAH showed a peak at 1780 cm^{-1}, which was attributed to the symmetric and asymmetric vibrations of C=O of acid anhydride. The peak at 1720 cm^{-1} was ascribed to the C=O of carboxylic acid, formed by the hydrolysis of anhydride. The FTIR spectra of PP-g-(AA-MAH), PP-g-AA, and PP-g-MAH fibers all showed peaks for stretching vibrations of C=O of the carboxyl group at 1720 cm^{-1}. The difference was that the FTIR spectrum of PP-g-(AA-MAH) had stronger intensity for C=O peak, indicating that its carboxyl content was higher than those of PP-g-AA and PP-g-MAH fibers. However, the FTIR spectrum of PP-g-(AA-MAH) fiber did not show peaks for symmetrical and asymmetrical vibrations of C=O of acid anhydride in the PP-g-MAH spectrum. This was due to the fact that MAH was grafted on to PP in the form of maleic acid[42,43]. FTIR results confirmed the successful grafting of AA and MAH onto PP fibers.

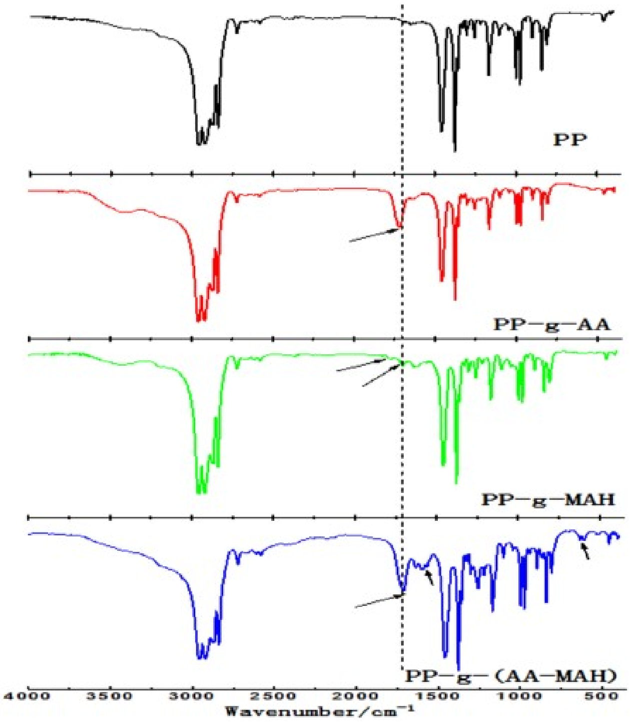

Figure 6. FTIR spectra of PP, PP-g-AA, PP-g-MAH and PP-g-(AA-MAH) fibers

3.5.2 ^{1}H-NMR analysis

The carboxyl group in PP-g-(AA-MAH) fiber was linked to -CH-. From the ^{1}H-NMR analysis (Figure 7), it was evident that compared with PP fiber, PP-g-(AA-MAH) fiber showed a chemical shift at around 2.3 ppm[43], indicating that the carboxyl groups were successfully grafted onto the surface of PP fibers.

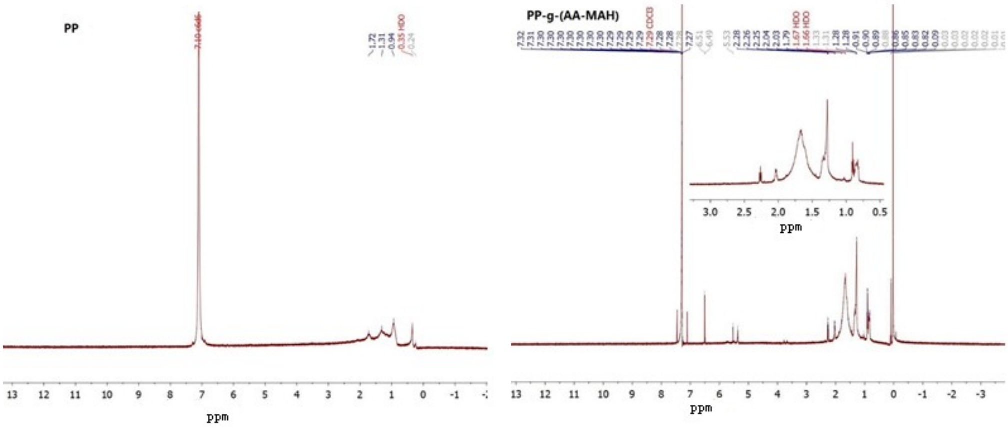

Figure 7. ^{1}H-NMR analysis of PP and PP-g-(AA-MAH) fibers

3.5.3 Analysis on hydrophilicity

Figure 8 showed a linear fitting relationship of $(\Delta P)^2$ of degreased cotton, PP-g-(AA-MAH) fiber and PP fiber with t. It could be seen from the figure that the K_0 of degreased cotton was 45.66, whereas K_θ of PP-g-(AA-MAH) fiber and PP fiber were 17.95 and 3.19, respectively. According to Eqn. 4, the calculated water contact angles of PP-g-(AA-MAH) fiber and PP fiber were 66.85° and 85.98°, respectively,

Preprints (www.preprints.org) | NOT PEER-REVIEWED | Posted: 27 August 2020 doi:10.20944/preprints202008.0599.v1

which indicated increased hydrophilicity of PP-g-(AA-MAH) fibers.

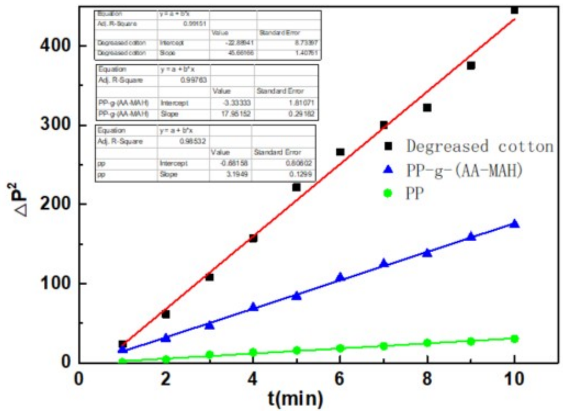

Figure 8. Linear fitting relationship of *$(\Delta P)^2$* of degreased cotton, PP-g-(AA-MAH) and PP fiber with t

3.6 Investigation of aniline-adsorption performance of PP-g-(AA-MAH) fiber before and after regeneration

Under the conditions of 25 °C, pH = 7, and initial aniline concentration of 300 mg/L, the adsorptivities of aniline on PP-g-(AA-MAH) fibers at different adsorption times were investigated. Thereafter, the regeneration performance of PP-g-(AA-MAH) fibers was investigated using the adsorption capacity and desorption ratio of regenerated fiber, as shown in Figure 9.

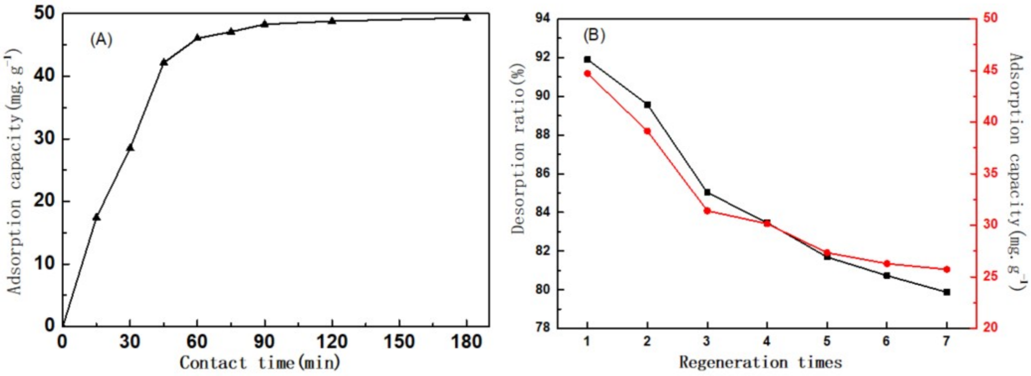

Figure 9. The adsorption capacity and desorption ratio of regenerated fiber

Figure 9A showed that PP-g-(AA-MAH) fibers had faster adsorptivity for aniline within the first 45 min, with adsorption capacity reaching up to 42.2 mg/g. Then, the adsorption capacity increased slowly until it reached saturation at 120 min. In aqueous solution, PP-g-(AA-MAH) fibers were deprotonated and negatively charged. Aniline was present in the form of $C_6H_5NH_3^+$, and so the adsorption between the two components was mainly electrostatic in nature[24,25]. The faster rate of adsorption within the first 45 min was the result of the large number of active sites on the surface of PP-g-(AA -MAH) fibers. With prolongation of adsorption time, the number of active sites on the surface of PP-g-(AA-MAH) fibers gradually decreased along with decrease in aniline concentration. As a result, the driving force for adsorption obviously weakened and the adsorption capacity increased slowly until it reached saturated adsorption.

It can be seen from Figure 9B that after seven adsorption-desorption cycles, the desorption ratio of the PP-g-(AA-MAH) fiber still remained above 80% and the adsorption capacity for aniline could still reach 25.72 mg/g, indicating that PP-g-(AA-MAH) fiber had good regeneration-adsorption performance.

4 Conclusions

With PP as the matrix, AA and MAH as functional monomers, PP-g-(AA-MAH) fiber was prepared by suspension grafting and melt-blown spinning technology. The technology can be easily scaled-up to industrial level and the fibers can be used to adsorb aniline from wastewaters. The maximum grafting ratio was 12.47% under the following optimal suspension grafting conditions: grafting time of 3 h, AA : MAH = 0.75, total monomer content of 55%, BPO content of 1.4%, xylene content of 6 mL/g PP, and deionized water content of 8 mL/g PP. Melt flow-rate and thermal analysis indicated that the suspension grafting product had good fluidity and thermal stability, and could be spun by melt-blown process. FTIR and NMR analyses showed that AA and MAH were successfully grafted onto PP fibers. The hydrophilicity of PP-g-(AA-MAH) fiber was enhanced. Therefore, the adsorption for aniline from wastewaters was fast and the adsorption capacity could reach up to 42.2 mg/g at 45 min. Moreover, the fibers had good regeneration performance.

Author Contributions: Conceptualization, Zhouyang Lian and Wuji Wei; Data curation, Jie Zuo, Hui Qian and Zhengwei Luo; Formal analysis, Hui Qian and Zhengwei Luo; Investigation, Yiyang Xu and Jie Zuo; Methodology, Zhouyang Lian, Yiyang Xu, Hui Qian and Wuji Wei; Writing – original draft, Zhouyang Lian, Hui Qian, Zhengwei Luo and Wuji Wei; Writing – review & editing, Zhouyang Lian..

Funding: This work was financially supported by the National Natural Science Foundation of China (Grant Number 21676144).

Acknowledgments: W.W.J. would like to thank the support from the Natural Science Foundation of China (Grant Number 21676144).

Conflicts of Interest: The authors declare no conflict of interest.

References

1. Pagalan, E.; Sebron, M. Activated carbon from spent coffee grounds as an adsorbent for treatment of water contaminated by aniline yellow dye. Ind. Crop. Prod. 2020, 145, 111953.
2. Reddy, M.C.S.; Nirmala, V. Bengal Gram Seed Husk as an adsorbent for the removal of dye from aqueous solutions – Batch studies. Arab. J. Chem. 2017, 10, S2554-2566.
3. Ferreiro, C.; Villota, N. An efficient catalytic process for the treatment of genotoxic aniline wastewater using a new granular activated carbon-supported titanium dioxide composite. J. Clean. Prod. 2019, 228, 1282-1295.
4. Koyuncu, H.; Kul, A.R. Removal of aniline from aqueous solution by activated kaolinite: Kinetic, equilibrium and thermodynamic studies. Colloid. Surface. A. 2019, 569, 59-66.
5. Dewage, N.B.; Liyanage, A.S. Fast aniline and nitrobenzene remediation from water on magnetized and nonmagnetized Douglas fir biochar. Chemosphere. 2019, 225, 943-953.

6. Bing, K.; Vakili, M. Adsorption of dyes by nanomaterials: recent developments and adsorption mechanisms. Sep. Purif. Technol. 2015, 150, 229-242.
7. Gupta, V.K.; Kumar, R. Adsorptive removal of dyes from aqueous solution onto carbon nanotubes: a review. Adv. Colloid Interface Sci. 2013, 193-194, 24-34.
8. Konicki, W.; Aleksandrzak, M. Adsorption of anionic azo-dyes from aqueous solutions onto graphene oxide: equilibrium, kinetic and thermodynamic studies. J. Colloid Interface Sci. 2017, 496, 188-200.
9. Benito, A.; Penades, A. Degradation pathways of aniline in aqueous solutions during electro-oxidation with BDD electrodes and UV/H_2O_2 treatment. Chemosphere. 2017, 166, 230-237.
10. Qi, Y.G.; Toyooka, T. Comparative γ-H2AX analysis for assessment of the genotoxicity of six aromatic amines implicated in bladder cancer in human urothelial cell line. Toxicol. In. Vitro. 2020, 66, 104880.
11. Tao, N.; Liu, G.Y. Genotoxicity and growth inhibition effects of aniline on wheat. Chemosphere. 2017, 169, 467-473.
12. Eskola, M.; Altieri, A. Overview of the activities of the European food safety authority on mycotoxins in food and feed. World. Mycotoxin. J. 2018, 11, 277-289.
13. European Commission, 2004. European Union Risk Assessment Report Aniline. Office for Official Publications of the European Communities, Luxembourg.
14. US EPA, O., 2014. Contaminant Candidate List 4-CCL 4. US EPA accessed 10.9.18. https://www.epa.gov/ccl/contaminant-candidate-list-4-ccl-4-0.
15. Gang, X.; Wang, Q. Simultaneous removal of aniline, antimony and chromium by ZVI coupled with H_2O_2: implication for textile wastewater treatment. J. Hazard Mater. 2019, 368, 840-848.
16. Qi, Y.F.; Guo, C. Co/Fe and Co/Al layered double oxides ozone catalyst for the deep degradation of aniline: Preparation, characterization and kinetic model. Sci. Total. Environ. 2020, 715, 136982.
17. Li, W.; Chen, C. Efficient removal of aniline by micro-scale zinc-copper (mZn/Cu) bimetallic particles in acidic solution: An oxidation degradation mechanism via radicals. J. Hazard Mater.2019, 366, 482-491.
18. Dvorak, L.; Lederer, T. Removal of aniline, cyanides and diphenylguanidine from industrial wastewater using a full-scale moving bed biofilm reactor. Process Biochem. 2014, 49, 102-109.
19. Gomez, J.L.; Leon, G. Application of reverse osmosis to remove aniline from wastewater. Desalination. 2009, 245, 687-693.
20. Wu, X.H.; Lei, Z.G. Liquid–liquid extraction of low-concentration aniline from aqueous solutions with salts. Ind. Eng. Chem. Res. 2010, 49, 2581-2588.
21. Li, C.H. Recovery of aniline from wastewater by nitrobenzene extraction enhanced with salting-out effect. Biomed. Environ. Sci. 2010, 23, 208-212.
22. Zhang, Q.; Zhang, W.L. Effects of dissolved oxygen concentrations on a bioaugmented sequencing batch rector treating aniline-laden wastewater: Reactor performance, microbial dynamics and functional genes. Bioresour Technol. 2020, 313, 123598.
23. Gan, Y.; Chen, G. Oxygen-rich hyper-cross-linked polymers with hierarchical porosity for aniline adsorption. Chem. Eng. J. 2019, 368, 29-36.

24. Gao, D.W.; Hu, Q. High-capacity adsorption of aniline using surface modification of lignocellulose-biomass jute fibers. Bioresour. Technol. 2015, 193, 507-512.
25. Li, H.Y.; Liu, L.X. High-efficiency adsorption and regeneration of methylene blue and aniline onto activated carbon from waste edible fungus residue and its possible mechanism. Rsc. Adv. 2020, 10, 14262-14273.
26. Huang, Q.; Hu, D.W. Sequential removal of aniline and heavy metal ions by jute fiber biosorbents: A practical design of modifying adsorbent with reactive adsorbate. J. Mol. Liq. 2019, 285, 288-298.
27. Chang, Y.; Ren, C. Preparation and characterization of Fe3O4/graphene nanocomposite and investigation of its adsorption performance for aniline and p-chloroaniline. Appl. Surf. Sci. 2012, 261, 504-509.
28. Sajab, M.S.; Chia, C.H. Cationic and anionic modifications of oil palm empty fruit bunch fibers for the removal of dyes from aqueous solutions. Bioresour. Technol. 2013, 128, 571-577.
29. Chai, W.B.; Liu, X.Y. Preparation and characterization of polypropylene fiber-grafted polybutylmethacrylate as oil sorbent. Desalin. Water Treat. 2016, 57, 18560-18571.
30. Mahtabani, A.; Rytoluoto I. On the Silica Surface Modification and Its Effect on Charge Trapping and Transport in PP-Based Dielectric Nanocomposites. ACS Appl. Polym. Mater. 2020, 2, 3148-3160.
31. Soylemez, M.A.; Barsbay, M. Preparation of well-defined erythromycin imprinted non-woven fabrics via radiation-induced RAFT-mediated grafting. Radiat. Phys. Chem. 2018, 142, 77-81.
32. Luo, Z.W.; Chen H.N. Surface grafting of styrene on polypropylene by argon plasma and its adsorption and regeneration of BTX. J. Appl. Polym. Sci. 2018, 135, 46171.
33. Guo, M.L.; Zhang C. An Efficient, Simple and Facile Strategy to Synthesize Polypropylene-g-(acrylic acid-co-acrylamide) Nonwovens by Suspension Grafting Polymerization and Melt-blown Technique. Fiber. Polym. 2016, 17, 1123-1130.
34. Luo, Z.W.; Xu, J.H. Ion-Imprinted Polypropylene Fibers Fabricated by the Plasma-Mediated Grafting Strategy for Efficient and Selective Adsorption of Cr(VI). Polymers-Basel. 2019, 11, 1508.
35. Chen, H.N.; Guo, M.L. Green and Efficient Synthesis of an Adsorbent Fiber by Plasma-induced Grafting of Glycidyl Methacrylate and Its Cd(II) Adsorption Performance. Fiber. Polym. 2018, 19, 722-733.
36. Liang, F.C.; Yuan, H. Study of suspension grafting process of polypropylene. Des. Monomers. Polym. 2018, 21, 130-136.
37. Z Li, Z.; Ma, Y.H. A Facile, Green, Versatile Protocol to Prepare Polypropylene-g-Poly(methyl methacrylate) Copolymer by Water-Solid Phase Suspension Grafting Polymerization Using the Surface of Reactor Granule Technology Polypropylene Granules as Reaction Loci. J. Appl. Polym. Sci. 2013, 129, 3170-3177.
38. Kyung, B.I.; Young, K.H. Development of a Melt-blown Nonwoven Filter for Medical Masks by Hydro Charging. Text. Sci. Eng. 2014, 51, 186-192.
39. Ji, L.Y.; Shi, B.L. A novel method for determining surface free energy of powders using Washburn's equation without calculating capillary factor and contact angle. Powder Technol. 2015, 271, 88-92.
40. Chang, Q.; Wei, B.G. Capillary pressure method for measuring lipophilic hydrophilic ratio of

filter media. Chem. Eng. J. 2009, 150, 323-327.

41. Wu, R.D.; Tong, X.L. Grafting PP by Swelling Suspension Copolymerization Process. China Plastics. 2002, 8, 64-68.
42. Wu, R.D.; Tong, X.L. Graft Copolymerization of Acrylic Acid onto Polypropylene by Suspension process. J. Functional Polym. 2001, 14, 85-89.
43. Zhou, Q.; Yang, P.D. Preparation of PP-g-MAH fiber using suspension grafting and its adsorption ability for copper ions in water. N. Chem. Mater. 2015, 43, 240-243.
44. Liang T.; Yan, K. Synthesis of a low-molecular-weight copolymer by maleic acid and acrylic acid and its application for the functional modification of cellulose. Cellolose. 2020, 27, 5665-5675.